DOI: 10.13009/EUCASS2017-301

Numerical Study of Flow Characteristics of the 14-X B Hypersonic Aerospace Vehicle Inlet with Blunted Leading Edge

Sergio N. P. Laitón, João F. A. Martos*, David Romanelli Pinto, Israel S. Rêgo**, Antonio C. Oliveira** and Paulo G. P. Toro***

**Instituto Tecnológico de Aeronáutica*

Praça Marechal Eduardo Gomes, 50 Vila das Acácias, 12228-900. São José dos Campos/SP – Brasil.

***Instituto de Estudos Avançados*

Trevo Coronel Aviador José Alberto Albano do Amarante, nº1, 12.228-001. São José dos Campos/SP – Brasil.

Abstract

The Brazilian hypersonic aerospace vehicle 14-X B is a technology demonstrator of a hypersonic air-breathing propulsion system, based on supersonic combustion ramjet (scramjet). It is designed for Earth's atmospheric flight at Mach number of 7 and an altitude of 30 km. Currently, it is under development in the Aerothermodynamics and Hypersonics Professor Henry T. Nagamatsu Laboratory at Institute for Advanced Studies (IEAv). Numerical simulations were conducted at nominal freestream Mach number and altitude for two leading edge blunting radius and several angles of attack close to horizontal flight. Initially, was selected the method of tip blunting around several types, the selection criteria were the location of shock wave, length of compression ramp and shock on-lip condition of all incident shock waves. The results show the shock interference behaviour on the blunted cowl-lip change with the angle of attack, blunted radius and method of tip blunting. Tip blunting by arc segment tangent to edge is the method that results in shock wave closer to cowl-tip. When the inlet operates in positive angles of attack higher to 1, no shock interference occurs, only the bow shock conditions. The results indicate a high air pressure at beginning of the combustor and higher pressure recovery with 2 mm radius and positives angles of attack.

1. Introduction

The Brazilian hypersonic aerospace vehicle 14-X B (Figure 1) is a technological demonstrator of a hypersonic air-breathing propulsion system, based on supersonic combustion ramjet (scramjet). It is designed for Earth's atmospheric flight at Mach number of 7 and an altitude of 30 km. under this flight conditions the kinetic energy of the air is converted to heat by compression and deceleration of flow. The heat is transfer from the high temperature air to vehicle surface.

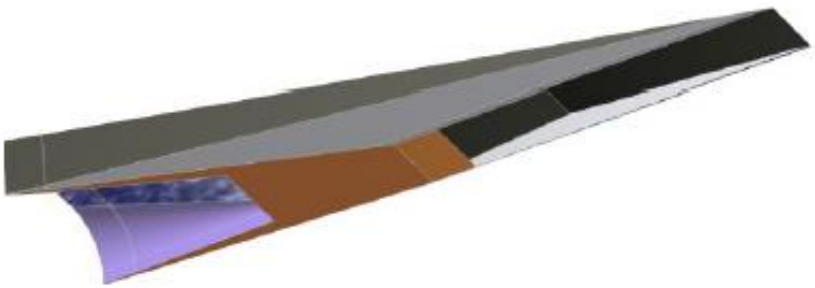

Figure 1: Hypersonic aerospace vehicle 14-X B.

The waverider concept, derived from a cone (Figure 2), is used in aerospace vehicles to be supported by tethered conical shockwave, originating on the leading edge of the aerospace vehicle and attached to the underside of the vehicle that generates a high-pressure zone, resulting in high lift and minimum drag. Waverider vehicles generate high lift-and-drag rates at high speeds (Mach number), producing superior aerodynamic performance compared to other concepts of hypersonic aerodynamics [1-3]. The atmospheric air pre-compressed by the shock wave, which is

DOI: 10.13009/EUCASS2017-301

comprised between the conical shock wave and the surface (inlet) of the vehicle can be used in air breathing hypersonic propulsion system based on the scramjet technology.

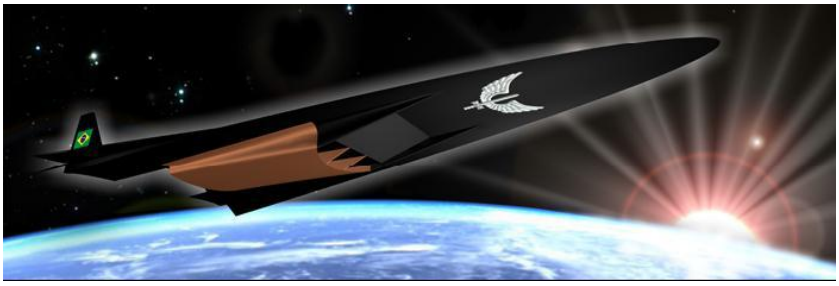

Figure 2: Aerospace hypersonic vehicle 14-X waverider.

The compression system is a critical component in the operation of the scramjet engine and the design has important effects on overall performance. The main function of this component is to capture the exact amount of air and to produce the necessary conditions of pressure, temperature and mass flow for the combustion process, while at the same time trying to reduce aerodynamic losses and total pressure with the lowest increase of entropy. The effectiveness of this component has direct effects on the performance of the later components of the engine (i.e. combustor, expansion section), so greater attention should be taken of the design of the compression system.

Generally, the compression system is designed from the characteristics of the mission of the vehicle to ensure operation in the desired range of the scramjet engine. Therefore, factors such as flight altitude, speed (Mach number) and angle of flight attack are important parameters to determine the performance of it. On the other hand, the strong structure-engine integration of the scramjet-integrated hypersonic vehicle must combine the inlet (the frontal surfaces of the vehicle) with the engine. The flow in the compression system is processed by oblique (conical or plane) shock waves formed from the external or internal surfaces of the engine and from the contraction of the component area.

The inlet of the scramjet engine is responsible for decelerating and delivering the airflow to the combustion chamber under the conditions suitable for combustion, within a wide range of engine operation. Under normal conditions the inlet must operate in the start mode, however in hypersonic vehicles a variation in the operating conditions causes the alteration of the shock wave system formed in the inlet, producing complex reflections inside of the combustion chamber, which increases the flow pressure to block the air passage by forcing the unstarted engine operation. Under these conditions the performance of the scramjet inlet drops drastically and the airflow becomes unstable [4, 5].

The hypersonic inlet is one key component for performance and operation of hypersonic airbreathing propulsion system. Due to several conditions of high temperature of hypersonic flight the sharp leading edge are necessarily blunting to avoid serious aero-heating problems. Hypersonic inlet of scramjet engine must capture and compress incoming air to engine operation. The main function is ensure the sufficient mass flow of air at conditions required for supersonic combustion at combustion chamber. This component is theoretically design for specific conditions. The shock structure into the inlet is well defined to study inlet performance. Mach number, altitude, angle of attack and blunting leading edge are factors those modified the shock structure producing shock reflections and spillage of mass at entrance of inlet, that deteriorate the inlet performance. Additionally, in term of manufacturing a sharp leading edge is not possible. Some blunted radius is needed in real conditions, which reduces the aerodynamic heating.

Due to operating characteristics the scramjet engine, the scramjet is fully integrated to the aerospace vehicle avoiding structural loads generated by engine-fuselage connections. This close relationship between engine-fuselage generates a variation of the longitudinal stability of the vehicle as a function of the performance of the propulsion system. The compression process, and consequently combustion and expansion depend on the operating conditions of the vehicle (altitude, Mach number and angle of attack), changing in the velocity, altitude or trajectory of the vehicle alters the engine performance.

In previous studies of 14-X B in T3 Hypersonic Shock Tunnel were found signs of ablation in the sharp edge region [6, 7]. In these experiments the inlet was designed and built with sharp leading edges of the vehicle and of the engine cowl, rigorously following the developed theoretical geometry. Due to the workpiece manufacturing methods, it is not possible to reach completely sharp edges and some level of rounding is considered in the test, in the case of experimental studies of vehicle 14-X B was considered approximately 1 mm radius.

DOI: 10.13009/EUCASS2017-301

To avoid aerodynamic heating problems at the leading edge of the vehicle, it is necessary to manufacture a blunted at the leading edge. The semi-spherical geometry in contact with the hypersonic flow generates a normal shock wave, that interacts with the oblique shock wave of the first inlet ramp. The interaction between the two waves produces an alteration in the structure of the shock waves of the inlet which depends mainly on the rounding radius and the flight Mach number. In this paper the numerical study of the rounding effects of the leading edge of the vehicle 14-X B. The influence on the structure of the shock waves of the inlet and its performance for different angles of attack are analyzed.

2. Blunting Leading Edge Methods

Considering the geometry of the 14-X B (Figure 3) different methods of rounding the leading edge of the vehicle was determined (Figure 4). The oblique shock waves produced by the inlet compression ramps are originate from the sharp leading edge and the deflection between the ramps, according to the original theoretical geometry. Shock waves strike directly at the sharp edge of the engine cowl. The rounding methods were analyzed considering minimum modifications in the original geometry by restricting the angles of the ramps of the inlet and the position of the engine cowl.

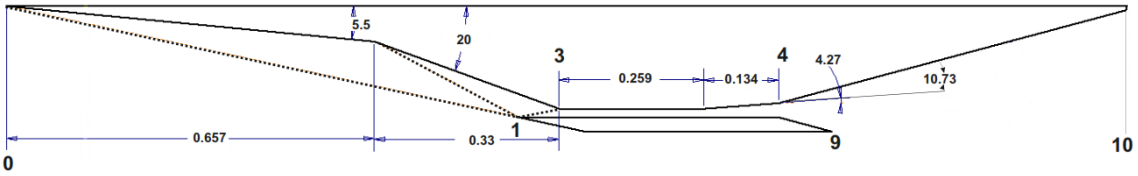

Figure 3: 14-X B geometry.

Three methods of vehicle leading edge rounding were studied (Figure 4). In all three cases it was used 1 mm radius at the leading edge. Two of rounding methods keep the original length of the model, which are defined as Radius Tangent Ramp, Radius Tangent Upper Chamber. In the first case the rounding radius (Radius Tangent Ramp) is tangent to the first ramp compression. Through this method the height of the vehicle increases to fit the radius of curvature. The second radius of rounding method (Radius Tangent Upper Chamber) the rounding radius is tangent the upper surface of the vehicle and it is shifting the position of the ramp to keep the length of the original model. In this case the height of the vehicle is not modified but the intersection, of the surfaces of the ramps, occurs on the second ramp at a point lower of the original geometry. In the third method, the rounding radius (Radius Tangent Internal) is a tangent curve segment located in the interior between the ramp surface and the extruder. The surfaces are cutting to engage the curve so the length of the pattern decreases. The other values of the original geometry are retained for this method.

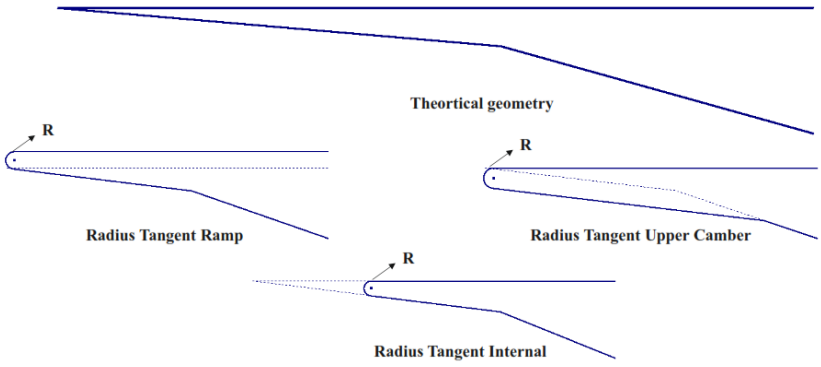

Figure 4: Theoretical geometry and blunting methods for 14-X B inlet.

The characteristics of the rounding methods are compared with the preliminary numerical analysis considering non-viscous flow. The objective of this analysis is to obtain a preliminary position of the shock waves generated in the inlet with the leading edge rounding. The analysis is performed numerically using the ANSYS Fluent software for aerodynamics of CFD computational flows. The based geometry used in the numerical analysis is shown in figure 5.

DOI: 10.13009/EUCASS2017-301

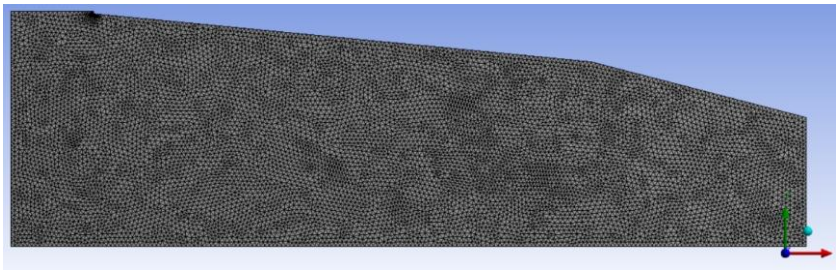

Figure 5: Geometry and computation grid.

Figure 6 shows the Mach number contour in the region of the inlet for the three of the rounding methods. In each case a normal shock wave is formed in the rounding region creating a subsonic flow zone. This flow is then accelerated parallel to the flow path on the ramps. With the generation of normal shock wave the oblique shock wave is displaced but with equal angle of the case with sharp leading edge.

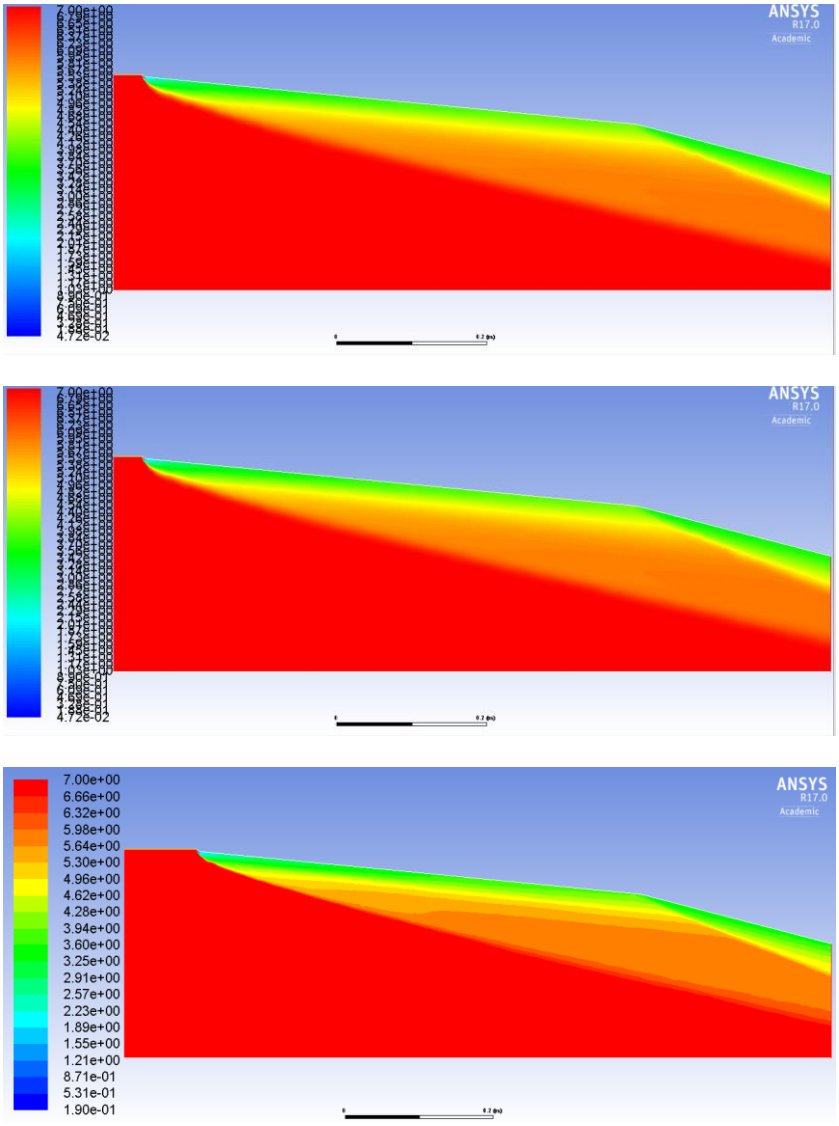

Figure 6: Mach Number contours for blunting methods. (upper view) Radius Tangent Ramp. (middle) Radius Tangent Upper Chamber. (bottom view) Radius Tangent Internal.

DOI: 10.13009/EUCASS2017-301

The displacement of the oblique shock wave of the Radius Tangent Ramp and Radius Tangent Internal methods are approximately equal (Figure 6). In both cases the wave is shifted downwards and does not intersect the cowl edge of the engine (no shock on lip condition).

For the second rounding method (Radius Tangent Upper Chamber) the oblique shock wave of the first ramp is clearly farther than the other two rounding methods (Figure 6 middle view). On the other hand length of the second ramp must be modified, in order to keep the original length of the inlet model and the shock wave generated in this deflection focus on the inner surface of the engine cowl, losing shock on-lip condition.

For the three rounding methods, the oblique shock wave of the first ramp is displaced due to the normal shock wave generated in the blunt region, so none of the cases under the conditions analyzed will match the on-lip shock condition. Considering the standard of the shock waves produced by the original geometry, the Radius Tangent Upper Chamber distance method completely changes the position of the shock waves of the inlet. However, the method needs minor changes in the inlet geometry, the great change of the inlet shock waves make it a non-viable alternative for application.

In terms of modification of the inlet shock waves, the Radius Tangent Ramp and Radius Tangent Internal methods have similar characteristics producing an approximately equal displacement. From a structural point of view of the inlet the Radius Tangent Ramp method needs a major modification of the original geometry compared to the Radius Tangent Internal method. This last method has better characteristics to perform a rounding of the model 14-X B.

3. Angle of Attack Analysis

With the variation of the angle of attack of the vehicle the positioning of the shock waves in the inlet is modified. To understand this variation and considering the rounding of the leading edge of the first ramp, a numerical analysis of the flow behavior under these conditions was carried out. For this analysis, the engine cowl is no longer considered with a sharp leading edge but using the Radius Tangent Internal method, so that the aerodynamic heating in this region is decreased.

The radius of rounding of the leading edge of the vehicle is varied to 1, 3 and 5 mm. For each radius the length of the vehicle is changed to fit the rounding curve. The geometry that is used in the analysis is shown in figure 7, in this case the front part of the cowl is included in the analysis to visualize the interaction of the waves with the variation of the angle of attack. For the rounding of the cowl the Radius Tangent Internal methodology with radius of 2 mm was used. In this way the engine cowl geometry has not been significantly altered and allows visualization of the position of the incident shock wave.

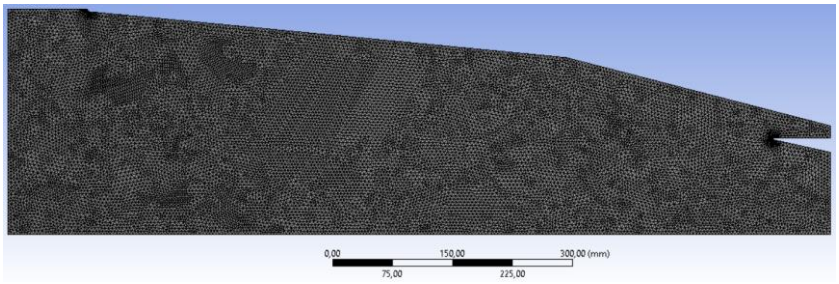

Figure 7: Geometry and computation grid with cowl tip profile.

A rounding radius is initially established and the angle of attack is varied around the horizontal position of the vehicle at positive and negative angles. Then the rounding radius is changed and again the variation of the angle of attack is performed. The angle of attack variation is limited between 5.5 ° and -5.5 ° according to the angle of the first ramp.

Considering a rounding radius of 1 mm from the vehicle leading edge the normal shockwave is formed and is coupled with the oblique shock wave from the first ramp. This interaction produces the detachment of the oblique shock wave resulting in the displacement of the intersection point at the height of the engine cowl. From the nominal horizontal position of the model, the angle of attack is positively varied in values of 3° and 5.5°. The contour of the Mach number through the model inlet is shown in Figure 8 as well as Mach number contours for negative angles of attack.

DOI: 10.13009/EUCASS2017-301

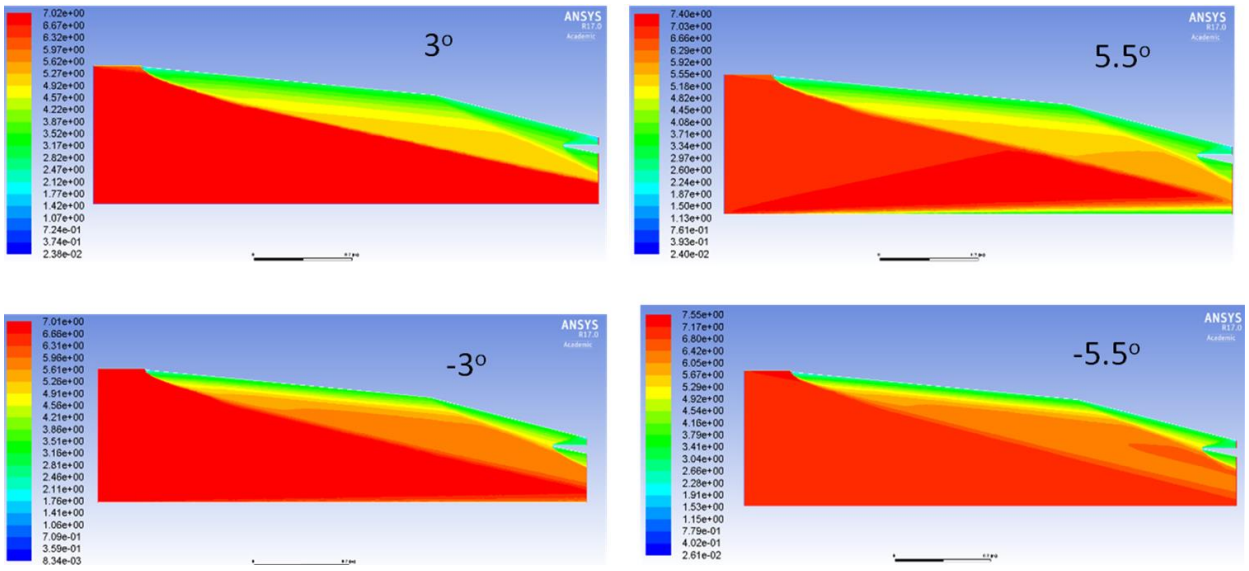

Figure 8: Mach number contours for AoA conditions (1mm radius at vehicle leading edge and 2mm radius at the cowl leading edge).

At positive angles of attack the angle of the shock wave of the first ramp increases therefore the shock wave is furthest from the edge of the cowl. For these cases it can also be observed that the shock wave of the second ramp increases its angle according to the increase of the angle of attack. Even if the rounding radius is small, it is sufficient to ward off the incident shock wave at any angle of attack condition.

For negative angles of attack the flow of the free stream realizes a smaller deflection in the first ramp because there is decrease of the angle of the ramp. Under these conditions the angle of the wave decreases with respect to horizontal reference of the flow however, the position of the shock wave of the first ramp is further away than the other conditions due to the rotation of the vehicle and negative angle of attack.

From the Mach number profiles the variation of the shock wave of the second ramp is observed. For positive angles of attack the wave is displaced towards the outside of the engine cowl, under these conditions none of the shock waves of the inlet has on-lip shock condition. For negative angles of attack a lower variation of the shock wave of the second ramp can be observed, the position of this wave varies around the edge of the engine cowl and interacts with the normal shock wave formed by the curvature of the surface. The interaction between the incident shock wave of the second ramp and the cowl normal shock wave produces important changes in the engine inlet section, which needed a more detailed analysis of this phenomenon. In the condition of angle of attack null can also be conserved this behavior (Figure 6).

Afterwards the analysis with radius of rounding of the leading edge of the model of 3mm and 5mm was carried out. The obtained results have similar behaviours for each radius of rounding. The influence of the rounding radius produces a larger normal shock wave for higher radius. This normal wave displaces the origin of the oblique shock wave generated on the first ramp, in this interaction the incident shock wave moves away from the deflection surface but with the same shockwave angle. Before the entrance of the combustion chamber there is a spillage of mass of air caused by the withdrawal of the shock wave from the first ramp. For larger rounding radii this spillage increases and holds for negative and positive angle of attack conditions.

Radius of roundness less than 1mm is difficult to reproduce with pressure in the experimental model due to the machining limits of the tools used. For rounding radii of 3mm or larger, the machining processes guarantee a certain level of precision. In the cases of experimental tests in wind tunnel the effect of the rounding can be visualized in cameras of high speed, through methods of visualization of flow based on the index of refraction of the means under study.

DOI: 10.13009/EUCASS2017-301

4. Results

The inlet of the 14-X B was theoretically studied with variation of the angle of attack (AoA) between -5.5º to 5.5º, with constant velocity and altitude as shown by the values in Table 1. The reason for the study varying only the AoA is analyzed considering that the longitudinal changes of the vehicle (pitching) occur in time intervals shorter than the time to change the trajectory or to vary the speed of the vehicle, in which cases also the behaviour of the input device.

Table 1: Free stream Conditions

AoA	M_0	p_0	T_0
0°	7	1197 [Pa]	226.5 [K]
-3°			
-5.5°			
3°			
5.5°			

In Figure 9 the position of each oblique shock wave generated by the inlet of the 14-X B, which were calculated under nominal design conditions, is plotted. It is possible identify two incident shock waves generated in the external compression section that converge in the cowl leading edge resulting in the on-lip condition. Also the reflected wave in the internal compression section converges in the on on-corner condition of the combustion chamber. As a first result of the calculation methodology used in this work was found a slight alteration of the position of the reflected shock wave as can be observed in Figure 8 losing the on-corner condition. This result was expected considering that the geometry and dimension used (Figure 3) considering the flow as a calorically perfect gas.

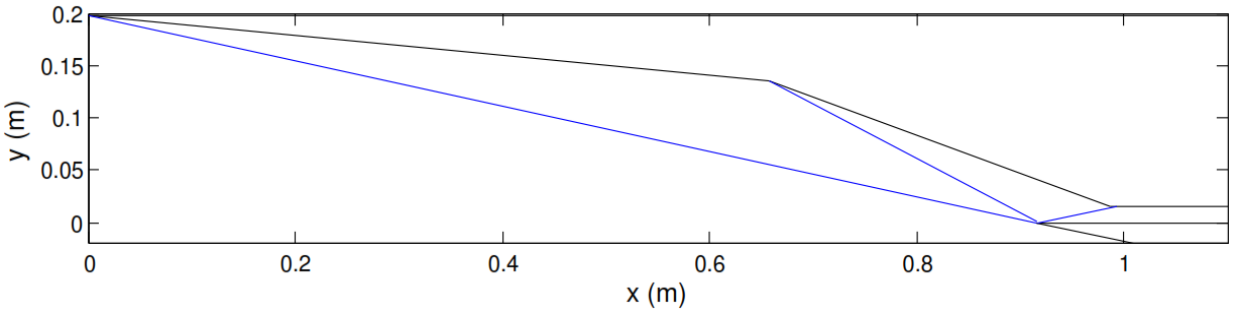

Figure 9: Nominal shock waves at 14-X B inlet.

Additionally, the flow behaviour in the inlet of the 14-X B for the nominal design conditions, presented through the pressure distribution, temperature and Mach number of the flow of Figures 10 and 11 were obtained. Observe the pressure and temperature curves can be identified a stepwise increase of properties as the flow advances in the inlet section, where each step represents the discontinuity that suffers the flow through each shock wave.

The shock wave reflected at the leading edge of the cowl engine is represented in each of the curves by the last step, at this point the flow undergoes a greater variation corresponding to an increase of the pressure and temperature, and a decrease of the Mach number, this indicates that the reflected shock wave is more intense in relation to the incident shock waves produced in the compression ramps. In percentages, the reflected shock wave produces 81% of the compression of the input device.

Figure 10 shows the pressure profile at isolator entrance of 14-X B under the AoA conditions studied. For negative AoA the effective deflection angle of the first ramp decreases relative to the free flow direction, in AoA condition of -5.5 the first ramp of the device is aligned with the direction of the free flow. Consequently there is no shock wave formation. Due to the decrease in effective deflection angle, the flow in the input device has a higher velocity generating sharper shock waves in the second ramp and in the fairing of the engine. In each case the reflected shock wave is displaced into the combustion chamber by losing the on-corner condition. Depending on the AoA (negative) the reflected shock wave affects more internally in the combustion chamber, provoking a new reflection of the wave that will move in the direction of the flow causing instability in the flow and altering the properties in the combustion chamber.

DOI: 10.13009/EUCASS2017-301

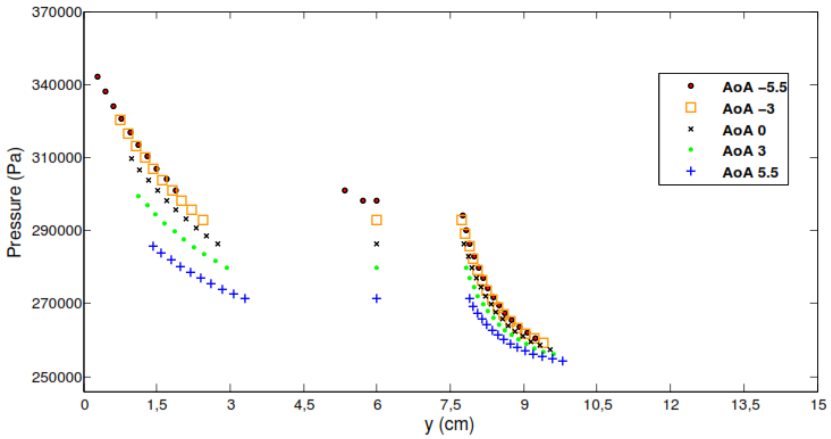

Figure 10: Pressure profile at isolator entrance.

Likewise, the shock wave of the second ramp, with no on-lip condition, and the reflected shock wave, are intercepted near the leading edge of the cowl engine, which may cause an alteration of the flow field. In either case the mass flow of air is altered causing spillage on the inlet of the vehicle. On the other hand, for positive AoA, the vehicle increases its exposure area to free flow, in the same way as increasing the effective deflection angle of the first ramp of the inlet of the vehicle. This results in a greater deceleration of the flow resulting in a more open shock wave for the second compression ramp. This situation generates the intersection of the shock waves in a region close to the leading edge of the cowl engine by losing the on-lip condition of the vehicle, as shown in Figures 10 and 11. After the intersection of waves, a resulting shock wave is formed passing beneath the engine cowl and a portion of the mass of air flow captured, proportional to AoA, is spilled near the leading edge of the fairing.

An interesting result is observed in the AoA condition of positive angle of 3º, where the reflected shock wave is in the on-corner condition (Figure 8), which implies that under these conditions the flow inside the combustion chamber must be stable and homogeneous. For the case of AoA of 5.5, the reflected shock wave impinges on the wall of the second ramp of the inlet of the vehicle, which can cause a train of expansion waves originating from the upper edge of the combustion chamber producing a region of complex flow behaviour.

Figure 11 shows the temperature distribution through the input device of the 14-X B under the AoA conditions studied. The curves present a similar profile of the compression process, but with different magnitudes for each AoA condition. The value of the magnitude of each of the curves is related to the variation of the effective deflection angle of the first ramp. Therefore, for negative AoA the pressure of the flow are lower than those obtained in design condition and for positive AoA these properties are higher. For the Mach number case the behaviour is completely opposite being higher for negative angles and lower for positive angles.

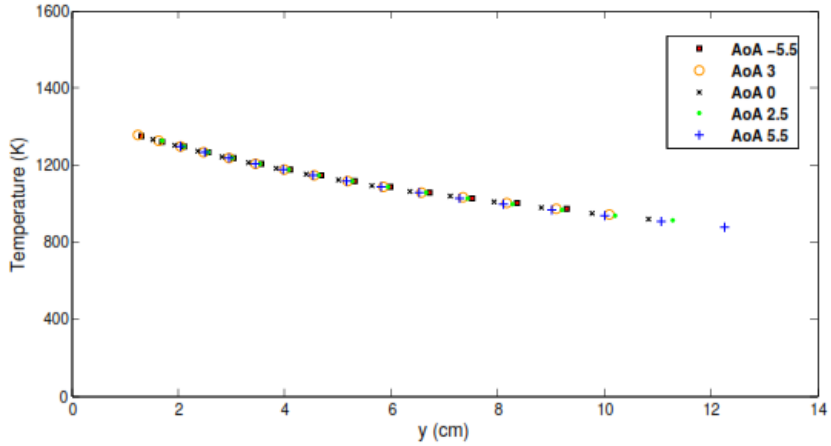

Figure 11: Temperature profile at isolator entrance.

Observing the temperature values at the combustion chamber entrance (station 3 of Figure 3), it can be seen that the results are in a much narrower range in relation to the pressure range of the different AoA conditions. Segal [8] points out the ignition time and the time to complete the combustion reactions are important limitations in the design of the

DOI: 10.13009/EUCASS2017-301

combustion chamber. Through a numerical calculation the author defines that the ignition distance depends largely on temperature for a given velocity and that the distance for the reaction depends heavily on the pressure and temperature. Consequently, the results obtained for the 14-X B inlet indicate that the length for the reactions may be a very unstable parameter under AoA conditions due to large variations in the pressure of the flow at the chamber entrance.

Figure 12 presents the parameters of spillage, air capture rate, recovery pressure factor and adiabatic kinetic energy efficiency of the inlet of the vehicle, for positive and negative angle of attack conditions. At zero angle of attack conditions the rate of air capture is maximum since the nominal catch area Ac is equal to the effective catch area A_0, therefore, in this condition there is no spillage in the inlet of the vehicle. The spillage curve shows that for positive angles of attack there is a greater air mass spill because in these conditions the shock wave produced by the first ramp is positioned farthest from the leading edge of the cowl engine. On the other hand, in the curve of $A_0 \,/\, Ac$ can be noted that for the condition of AoA -5.5 ° the air capture efficiency is maximum, as for AoA 0º, however, the mass air flow in the combustion is not the same in both cases, in fact, for AoA -5.5 ° the mass flow is less due to the decrease in the nominal area of the compression section A_0 and the effective capture area Ac as shown by the graphs of Figure 12.

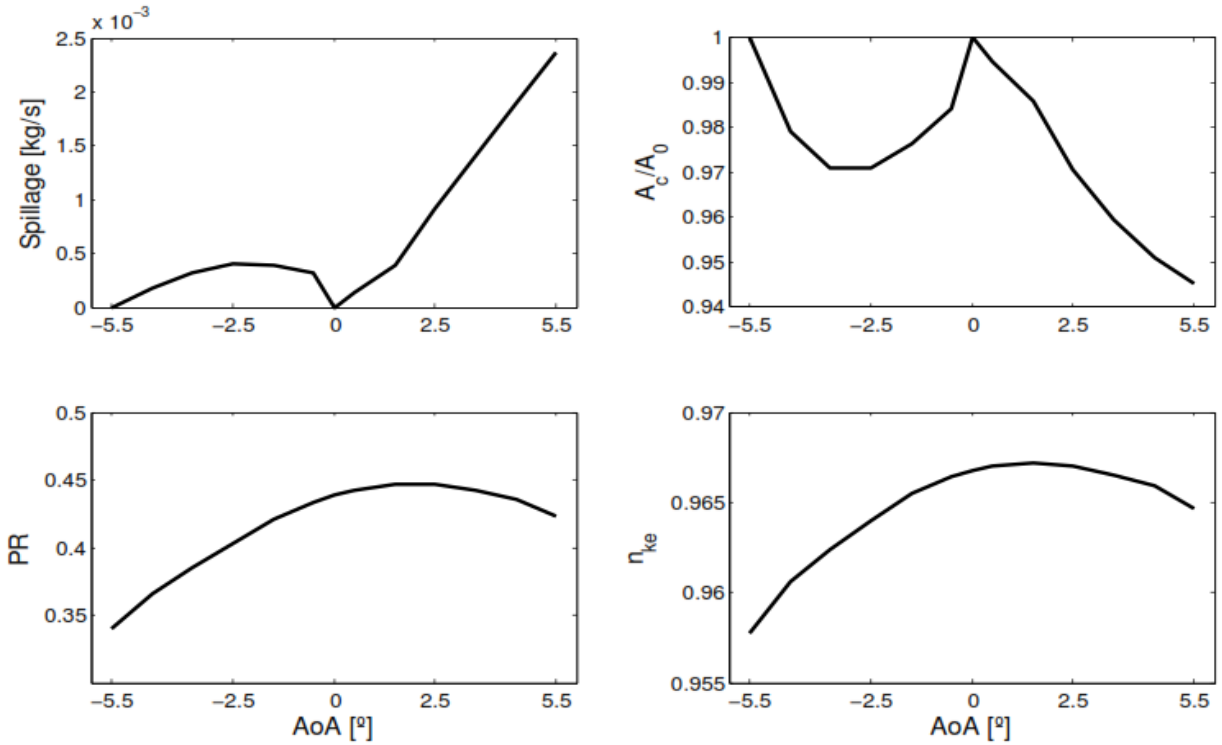

Figure 12: Efficiency parameters of 14-X B inlet in function of AoA.

Additionally, the performance curve of the recovery factor PR shows the condition of AoA -5.5° as the condition with the highest total pressure loss, and AoA condition of 3° with better compression efficiency, above the efficiency of the condition of project. At higher positive angles of attack, the recovery factor gradually decreases. This same behaviour is observed in the results of adiabatic kinetic energy efficiency, but with much higher values of efficiency.

5. Conclusions

The airflow through the 14-X B inlet was numerically analyzed under positive and negative angle of attack conditions for various rounding radius of the leading edge of the model. The performance of the inlet of the vehicle was evaluated through the flow properties at the combustion chamber entrance and the efficiency parameters of air capture rate, recovery pressure factor and adiabatic kinetic energy efficiency. The results show AoA condition of 3° with better compression efficiency, above the efficiency of the project condition. For AoA condition of 3° the reflected shock wave is in the on-corner condition. The properties of the flow through the input device vary in relation to AoA, being greater for positive angles and smaller for negative AoA. The results show the shock interference behavior on the blunted cowl-lip change with the angle of attack, blunted radius and method of tip blunting. Tip blunting by Radius Tangent Internal to edge is the method that results in shock wave closer to cowl-tip. When the inlet operates in positive angles of attack higher to 1°, no

DOI: 10.13009/EUCASS2017-301

shock interference occurs, only the bow shock conditions. The results indicate a high air pressure at beginning of the combustor and higher pressure recovery with 2 mm radius and positives angles of attack.

References

[1] Rault, D. F. G. 1994. Aerodynamic characteristics of a hypersonic viscous optimized waverider at high altitudes. *Journal of Space and Rockets. 31:719-727.*

[2] Rasmussen, M. L. 1994. Hypersonic flow. *Wiley-Interscience.*

[3] Rasmussen, M. L. 1990. Analysis of cone-derived waveriders by hypersonic small-disturbance theory. *First International Hypersonic Waverider Symposium*.

[4] Scott, D. H. 1994. Wind-tunnel blockage and actuation systems test of a two-dimensional scramjet inlet unstart model at Mach 6, *NASA-TM-10915.*

[5] Heiser, W. H. e Pratt, D. T. 1994. Hypersonic Airbreathing Propulsion, Washington D.C.: *American Institute of Aeronautics and Astronautics.*

[6] Galvao, V. 2016. Investigação Experimental do Demonstrador Tecnológico *scramjet* 14-x b em diferentes ângulos de ataque com Número de mach 7. Master disertation. Instituto Tecnológico de Aeronáutica, Programa de Pós-Graduação em Ciências e Tecnologias Espaciais

[7] C. Segal, The Scramjet Engine Processes and Characteristics, new York: Cambridge University Press, 2009.